

Environmental impact of fireworks during the celebration of New Year's Eve on the air quality in an urban region: Queretaro, Mexico

Alejandro Rodríguez-Trejo

`alexrt@geociencias.unam.mx`

Instituto de Geociencias, Laboratorio de Paleomagnetismo de Rocas. Universidad Nacional Autónoma de México

Héctor Enrique Ibarra-Ortega

Instituto de Geociencias, Laboratorio de Paleomagnetismo de Rocas. Universidad Nacional Autónoma de México

Harald Böhnel

Instituto de Geociencias, Laboratorio de Paleomagnetismo de Rocas. Universidad Nacional Autónoma de México

Reneé González-Guzmán

Instituto de Geociencias, Universidad Nacional Autónoma de México

Luis Enrique Sánchez-Ramos

Instituto de Geociencias, Universidad Nacional Autónoma de México

Ana Gabriela Castañeda-Miranda

Posgrado en Ingeniería para la Innovación Tecnológica, Unidad Académica de Ingeniería Eléctrica, Universidad Autónoma de Zacatecas

Victor Hugo Márquez-Ramírez

Instituto de Geociencias, Universidad Nacional Autónoma de México

Marcos Adrián Eduardo Chaparro

UNCPBA-CICPBA-CONICET

Mauro Alejandro Eduardo Chaparro

Centro Marplatense de Investigaciones Matemáticas (UNMDP-CIC), Facultad de Ciencias Exactas y Naturales (UNMDP)

Research Article

Keywords:

Posted Date: May 3rd, 2024

DOI: <https://doi.org/10.21203/rs.3.rs-4214257/v1>

License:  This work is licensed under a Creative Commons Attribution 4.0 International License.

[Read Full License](#)

Additional Declarations: No competing interests reported.

1 **Environmental impact of fireworks during the celebration of New Year's Eve on the**
2 **air quality in an urban region: Queretaro, Mexico**

3
4 **Rodríguez-Trejo, A.^{1,*}, Ibarra-Ortega, H.E.¹, Böhnel, H.¹, González-Guzmán, R.²,**
5 **Sánchez-Ramos, L.E.², Castañeda-Miranda, A.G.³, Márquez-Ramírez, V.H.²,**
6 **Chaparro, Marcos A.E^{4,5}, Chaparro, Mauro.A.E⁶**

7
8 *¹ Instituto de Geociencias, Laboratorio de Paleomagnetismo de Rocas. Universidad*
9 *Nacional Autónoma de México. Juriquilla, Querétaro, México. 76230*

10 *² Instituto de Geociencias. Universidad Nacional Autónoma de México. Juriquilla,*
11 *Querétaro, México. 76230*

12 *³ Posgrado en Ingeniería para la Innovación Tecnológica, Unidad Académica de Ingeniería*
13 *Eléctrica, Universidad Autónoma de Zacatecas, Zacatecas 98000, Zacatecas, México.*

14 *⁴ Centro de Investigaciones en Física e Ingeniería del Centro de la Provincia de Buenos Aires*
15 *(CIFICEN), UNCPBA-CICPBA-CONICET, Pinto 399, Tandil 7000, Argentina*

16 *⁵ IFAS, Facultad de Ciencias Exactas, Universidad Nacional del Centro de la Provincia de*
17 *Buenos Aires (UNCPBA), Pinto 399, Tandil 7000, Argentina*

18 *⁶ Centro Marplatense de Investigaciones Matemáticas (UNMDP-CIC), Facultad de Ciencias*
19 *Exactas y Naturales (UNMDP), Deán Funes 3350 (B7602AYL) Mar del Plata, Buenos Aires,*
20 *Argentina .*

21

22 *Corresponding author: alexrt@geociencias.unam.mx

23 ORCID: 0000-0002-6849-1876

24

25

26

27 **Abstract**

28

29 The high concentrations of particulate matter (PM) in the atmosphere have adverse effects
30 on both the environment and human health, as well as on urban and faunal biodiversity. Short-
31 term events, such as the burning of fireworks, attributable to human activity, result in a
32 significant and rapid increase in PM concentration levels within the atmosphere. We present
33 findings derived from observations made using low-cost PM sensors deployed as part of the
34 Environmental Monitoring Network in Querétaro, Mexico. These sensors utilize the
35 Environmental Geo Monitoring Stations (EMGA) device, developed by the Institute of
36 Geosciences at UNAM. The observation period spanned from December 10, 2023, to January
37 10, 2024, encompassed the Christmas and New Year holidays, and focused on PM_{2.5}
38 concentrations, and a comparison with a similar period from February 10, 2024, to March
39 10, 2024, considered a typical activity period in the area. The results reveal a substantial
40 increase in PM_{2.5} concentrations over time and spatial distribution during this period, with
41 notable increases observed during the festive season. Specifically, prolonged periods
42 exceeding up to 6 hours were noted on festivities dates. This research offers insight into the
43 effects, trends, and spatial-temporal distribution of pollutants within the city of Queretaro,
44 which may be used as a reference for other cities around the world. Furthermore, a
45 comparison between PM_{2.5} data recorded by the EMGA devices and infrasound data was
46 conducted complementarity to explore potential correlations between these two types of data.

47

48

49 **1. Introduction**

50 Fine Particulate Matter (PM) with an aerodynamic diameter of less than 2.5 μm ($\text{PM}_{2.5}$) has
51 garnered global attention due to its effects on air quality, human health, and climate (Li et al.,
52 2016). Under normal atmospheric circumstances, natural dust constitutes the primary
53 component of $\text{PM}_{2.5}$, however, in urban areas, it also contains significant concentrations of
54 inorganic and organic components, including black carbon, Potentially Toxic Elements
55 (PTE), and Polycyclic Aromatic Hydrocarbons (PAH) (Chen et al., 2022; Feng et al., 2019;
56 Li et al., 2016), all of which pose health risks. Once emitted into the atmosphere, this complex
57 mixture of pollutants can transform aerosols based on ambient conditions and interactions
58 among $\text{PM}_{2.5}$ components and air as well as gaseous pollutants (e.g., SO_x , NO_x , CO_x , and
59 volatile organic compounds). The atmospheric particulate system is particularly intricate in
60 urban areas due to (i) large emissions volumes of $\text{PM}_{2.5}$ components, (ii) gasses released by
61 anthropogenic sources, (iii) widespread distribution of emission sources, (iv) and climate.
62 Hence, it is crucial to monitor short-term events to identify dates and spatial patterns of
63 pollutant sources for environmental management and risk assessment (Chen et al., 2022;
64 Chhabra et al., 2020). Although technological sensors provide detailed information on PM
65 concentration over time, complementarily, environmental networks using biological
66 indicators can also provide particle pollution data recorded over months, years, or seasons
67 (McIntosh et al., 2007; Paoli et al., 2017; Castañeda Miranda et al., 2020; Chaparro et al.,
68 2024).

69

70 New Year's Eve is among the globally celebrated festivals as it marks the transition from the
71 old year to the new year in the Gregorian calendar. In major cities, such celebrations directly
72 impact the local environment, particularly the air quality (Lin, 2016; Ambade, 2018). The

73 bursting and burning of firecrackers during festivities release substantial concentrations of
74 $PM_{2.5}$ and gasses into the atmosphere. Previous studies have documented the adverse effects
75 of fireworks on air quality worldwide, for example, the significant increase in $PM_{2.5}$ levels
76 during the Diwali festival in India due to fireworks (Ambade, 2018). Moreover, there are
77 regional and global effects of this anthropogenic activity, as the resultant atmospheric
78 aerosols can alter Earth's climate balance through direct (scattering and absorption of solar
79 and longwave radiation), semi-direct (evaporation of cloud droplets due to solar absorption),
80 and indirect (modification of cloud optical properties, lifetime, and albedo) influences
81 (Chhabra et al., 2020).

82

83 The primary objective of burning fireworks as a recreational activity is to produce sound,
84 gasses, and smoke effects. Most common pyrotechnic mixtures comprise an oxidizer, a fuel,
85 a source of carbon, and various additives such as chlorine donors to enhance color and other
86 chemicals to modify appearance or sound (Rossol, 2014). Compounds affecting human
87 health, such as hazardous pollutants (e.g., $PM_{2.5}$ or dust), toxic gasses (SO_x , NO_x), and almost
88 any PTE, can be present in pyrotechnic emissions. The use of commercial low-cost
89 monitoring devices, such as Purple Air sensors, Smart Citizen Kit (Ardon-Dryer, et al., 2020;
90 Barkjohn et al., 2020; Camprodon et al., 2019; Farooqui et al. 2023), both devices using the
91 Plantower PMS5003 sensor, have created new opportunities for local and regional air quality
92 monitoring. Although less precise than traditional monitoring equipment, these devices
93 provide a cost-effective and accessible solution for environmental surveillance, enabling
94 increased citizen participation in data collection and decision-making. Studies like those
95 conducted have demonstrated the usefulness and feasibility of low-cost $PM_{2.5}$ sensors in
96 monitoring air quality, providing valuable data for understanding air pollution and its impact

97 on public health and environmental policies (Stravoulas et al., 2020; Mousavi et al., 2021;
98 Farooqui et al. 2023). This study aims to measure and analyze changes in PM_{2.5} concentration
99 during the intense pyrotechnic burning activity on Christmas and New Year's Eve in
100 Querétaro City (Mexico), using low-cost PM_{2.5} sensors. This research will contribute to a
101 better understanding of fireworks' impact on urban air quality and may provide valuable
102 information for designing and implementing public policies aimed at mitigating their adverse
103 effects.

104 **2. Materials and methods**

105

106 *2.1 Study area*

107 The study was conducted in the urban area of Santiago de Queretaro City and its Metropolitan
108 Area (Figure 1), which serves as the primary industrial and commercial hub of the El Bajío
109 region. A macroregion located within the central Mexican plateau, approximately 250 km
110 northwest of the Mexico City megalopolis. Queretaro's urban area is situated on a plain at an
111 elevation of 1900 meters above sea level. The urban area is home to approximately 1.5
112 million inhabitants (INEGI, 2020), concentrated across three municipalities: (i) Querétaro,
113 (ii) Corregidora, and (iii) El Marqués. The study area experiences a semi-arid climate (BSh),
114 classified in Köppen climate classification. The average annual temperature ranges from up
115 to 15 to 22°C, with an average annual precipitation *ca.* 528 mm.

116

117 The city hosts significant industrial activity, with around 28 industrial parks scattered
118 throughout the metropolitan area. Moreover, owing to its strategic central location within the
119 country, Queretaro serves as a major transportation hub, experiencing heavy traffic of cargo
120 transport vehicles bound for Mexico City and other regions, as well as substantial local

121 vehicle traffic. Industrial operations and the high volume of vehicular traffic represent
122 potential sources of atmospheric pollutants, which vary depending on temporal and
123 geographical variations in human activity. In addition, Queretaro is immersed in a heavily
124 industrial and agricultural region towards the west, which can contribute to the air pollutants
125 measured in its atmosphere.

126

127 *2.2 Instrumentation and data acquisition*

128 In-situ measurements were gathered from 11 stations within the Environmental Monitoring
129 Network of the Metropolitan Area of Queretaro City (Table 1) initiated by the Instituto de
130 Geociencias-Universidad Nacional Autonoma de Mexico, shown in Figure 1. This network
131 is comprised of Environmental Geo Monitoring Stations (EMGA) designed and developed
132 by the CGEO-UNAM, which continuously monitor eight environmental variables in real-
133 time: Particulate Matter (PM): PM_{2.5}, PM₁₀, and PM₁ concentrations in $\mu\text{g}/\text{m}^3$, temperature,
134 atmospheric pressure, relative humidity, environmental noise, and intensity of the Earth's
135 magnetic field. Data is collected every 4 minutes and promptly transmitted to a data
136 processing, storage, and visualization platform via the Internet. All EMGAs are installed
137 outdoors, typically near streets, at an average height ranging from 2 to 3 meters above ground
138 level. For this study, PM concentration data were specifically obtained on the particulate
139 matter at sizes of 2.5 μm determined in $\mu\text{g}/\text{m}^3$, as well as temperature and relative humidity,
140 continuously recorded over a period of up to 30 days spanning from December 10, 2023, to
141 January 10, 2024. As a comparison with a similar period from February 10, 2024, to March
142 10, 2024, considered a typical activity period in the area were performed.

143 The EMGAs use a commercial low-cost Plantower PMS5003 optical particulate matter
144 sensor for sizes of 2.5, 10, and 1 μm where their concentrations are determined in $\mu\text{g}/\text{m}^3$. The

145 use and performance of these sensors have been scrutinized and discussed by various
146 researchers (e.g., Kuula et al., 2020; Giordano et al., 2021; Kaur et al., 2023; Searle et al.,
147 2023), who propose diverse methodologies for evaluating their accuracy and precision. The
148 reliability of the data obtained with these sensors is subject to debate, particularly when
149 compared with high-precision reference equipment. Nonetheless, multiple studies agree that
150 data obtained from these sensors, although lacking the precision of high-performance
151 equipment, are valuable as references for detecting atmospheric pollutants. Unlike high
152 precision equipment, which incurs substantial installation and maintenance costs, these
153 sensors, due to their affordability, facilitate the establishment of dense air quality monitoring
154 networks at a reduced expense, enabling the observation of spatial discrepancies and seasonal
155 variations in urban environments. These sensors are the ones integrated into low-cost
156 commercial equipment networks like Purple Air, which boasts thousands of devices installed
157 across the USA, with their performance and validity assessed in various studies (Ardon-Dryer
158 et al., 2020; Barkjohn et al., 2020; Stavroulas et al., 2020; Farooqui et al. 2023).

159

160 In this study, raw mass concentration ($\mu\text{g}/\text{m}^3$) data were selected from each sensor for $\text{PM}_{2.5}$
161 with raw data collected every 4 minutes on the original time series. The data series underwent
162 hourly averaging for each sensor, followed by the application of a correction factor per hour
163 to mitigate the standard error of underestimation in the sensor model, described by Searle et
164 al. (2023). Subsequently, an statistical analysis was conducted with an algorithm, applied to
165 the data series to filter out outliers, excluding from the calculation of hourly averages any
166 data points that deviated beyond a σ (sigma) of the standard deviation of the data set. This
167 process effectively eliminated outlier data from the time series, enhancing its quality and
168 reliability, eliminating less than 10% of the data.

169 Additionally to the EMGA network, a network of 5 infrasound sensors was installed in the
170 City of Queretaro. The infrasound stations are equipped with Raspberry Shake Boom
171 instruments. These instruments have a flat response ranging from 0.1-50Hz, and sampling
172 rate of 100Hz. All the data is transmitted in real-time to the Institute of Geosciences and is
173 managed using the Seiscomp software. The objective of the infrasound network is monitoring
174 urban noise at infrasound and audible levels in the metropolitan area of Querétaro. Infrasound
175 data could be used as a source of comparison for human activity and the incidence of
176 environmental changes from anthropogenic origin and could be compared with data collected
177 from the EMGA stations.

178

179 **3. Results**

180

181 *3.1 Time series*

182 For the time series analysis and for comparison, three reference points were selected (Figure
183 2): the station with the highest values (STATION-10), a station with intermediate values
184 (STATION-19), and the station with the lowest values (STATION-13). Additionally, a
185 comparison was made with a time series from the station with the highest values recorded in
186 this study, but for a subsequent period of equal duration. This was done to establish a pattern
187 of variation among the spatially obtained results.

188

189 Figures 2a and 2b, corresponding to STATION-10 and STATION-19, depict the temporal
190 records of hourly averages, exhibiting typical variations for different days of the week, with
191 PM_{2.5} values averaging below 50 µg/m³. The blank spaces represent periods during which
192 the equipment did not record data attributable to specific site-related issues. Within the time

193 series, two peaks are evident, showing a significant increase during the early hours of
194 December 25, 2023, and January 1, 2024, considerably exceeding $150 \mu\text{g}/\text{m}^3$ and $300 \mu\text{g}/\text{m}^3$,
195 respectively. These increases persist for at least 6 hours during these specific events. These
196 peaks align with the Christmas and New Year festivities, with the elevated $\text{PM}_{2.5}$ recordings
197 directly linked to fireworks burning in the vicinity. During these times and dates, traffic and
198 industrial activity (among other factors) do not substantially contribute to $\text{PM}_{2.5}$ generation
199 in the environment, with average $\text{PM}_{2.5}$ concentrations below $30 \mu\text{g}/\text{m}^3$.

200

201 Figure 2c illustrates the time series for STATION-10 from February 10 to March 10, 2024,
202 displaying peaks with high $\text{PM}_{2.5}$ concentration values, albeit sustained for no more than 30
203 minutes. These peaks are primarily associated with traffic activity, and sustained increases
204 over several hours, as observed during the previously mentioned dates and times, are not
205 apparent. Figure 3 presents a comparison among three stations with the highest, intermediate,
206 and lowest values (STATION-10, STATION-19, and STATION-13, respectively). For
207 STATION-10 and STATION-19, a similar trend of increased $\text{PM}_{2.5}$ concentration was
208 observed, albeit in varying proportions, on December 25, 2023, and January 1, 2024.

209

210

211 *3.2 Meteorological conditions and $\text{PM}_{2.5}$ relationship*

212 As shown in Figure 4a, the comparison between the time series of the data record from
213 STATION-10 and the temperature record, where the temperature has a similar behavior
214 during this period, varies from 10°C to 20°C during the day. No specific dependence on the
215 significant increase in $\text{PM}_{2.5}$ concentrations is observed for December 25 and January 1.
216 Furthermore, during the period studied, there was no rainfall, and wind speeds varied within

217 a range of 0-40 km/h. Figure 4b shows no variation associated with changes on humidity
218 records are related to the increasing of the PM_{2.5} concentrations. This suggests that the abrupt
219 increase in these values is not correlated with a natural phenomenon (meteorological
220 conditions), indicating that the high concentrations of PM_{2.5} recorded are of an anthropic
221 origin, associated with the firework burning.

222

223 *3.3 Daily trends*

224

225 Based on the typical patterns of PM_{2.5} emission into the atmosphere, the results were grouped
226 by day of the week to examine the daily impact of human activities on PM_{2.5} levels in the
227 city. This involved estimating hourly averages and filtering out outliers, as previously
228 described. The data were then organized by day of the week, from Monday to Sunday, and
229 further segmented by time of day, from 0 a.m. to 11:59 p.m.

230

231 Figure 5d illustrates the daily PM_{2.5} records from February 10 to March 10, 2024,
232 representing typical activity patterns over four consecutive weeks. The graph highlights the
233 days of the week that, on average, contribute to higher levels of PM_{2.5} in the environment,
234 with notable peaks corresponding to peak traffic hours in the city.

235

236 In contrast, Figures 5a and 5b, representing STATION-19 and STATION-10 respectively,
237 depict a notable increase in PM_{2.5} concentration during the late hours of Sunday and the early
238 hours of Monday. This pattern coincides with observations in the time series of the same
239 stations during events characterized by high pyrotechnic activity. Figure 5c, showing the

240 lowest records for the studied period, exhibits a similar trend to Figure 5d, indicating that
241 pyrotechnic activity in this area was lower and less significant.

242

243

244 *3.4 Hourly trends*

245

246 To understand the specific variations per day for each station according to the time of day,
247 the same methodology of averaging within 1-hour intervals was employed. The results were
248 graphed in polar form, enabling visualization of hourly variations from 0 to 11:59 p.m. for
249 each day within the date range of this study.

250

251 Figures 6a and 6b depict the polar graphs illustrating the hourly behavior of stations
252 STATION-10 and STATION-19, respectively. Two curves can be observed, with a noticeable
253 increase from 9 p.m. to 11 p.m. on one curve, representing data from a single day. This
254 increase continues into a new curve, corresponding to a new day, from 0 to around 7 a.m.
255 This period coincides with the initiation of pyrotechnic burning from 9 p.m. on December
256 24, 2023, continuing until around 7 a.m. on January 2, 2024. This aligns with observations
257 from the comparison of time series data for the study period. Figure 6c displays the polar
258 projection for the STATION-13 sensor, which recorded the lowest concentration of PM_{2.5}
259 during the studied period. As shown in Figure 6, the burning of pyrotechnics was
260 considerably lower compared to other stations in the city. Figure 6d shows the polar
261 projection for the period between February 10, and March 10, 2024. Although the daily trends
262 differ from those of the STATION-13 station, as they correspond to different social
263 environments, a similarity in maximum averages can be observed. Neither of the two

264 projections exhibits sustained peaks for several hours, as observed in STATION-10 and
265 STATION-19.

266

267 *3.5 Histograms*

268

269 To observe the statistical impact of these short-term events, which nonetheless have a high
270 environmental significance (Gouder & Monterfort, 2014; Lin, 2016), histograms were
271 constructed for each station within the period of this study. PM_{2.5} concentrations were
272 grouped into ranges of PM_{2.5} concentration of 5 µg/m³ each. A Gaussian (normal) distribution
273 curve was fitted to the histogram to show the distribution of occurrence density for each
274 PM_{2.5} concentration range.

275

276 Figures 7a, 7b, and 7c present the histograms for stations: STATION-19, STATION-10, and
277 STATION-13, respectively, over the timeframe period. It is observed that in STATION-19
278 and STATION-13, the distribution of PM_{2.5} concentrations extends up to 40 and 50 µg/m³,
279 with very similar distributions. In the case of station STATION-10, concentrations extend up
280 to 50 and 60 µg/m³, with its distribution, although slightly higher, still similar to that of
281 STATION-19 and STATION-13. Figure 7d illustrates the histogram of data recorded between
282 February and March 2024 for station STATION-10, representing ordinary human activity. A
283 distribution with a similar trend is observed, but the 95% limits are reduced to 40 and 50
284 µg/m³. This demonstrates that in longer time series, these short-lived events become diluted
285 and challenging to detect, yet their environmental impacts remain significant.

286

287

288 *3.6 Spatial distribution of PM_{2.5}*

289

290 The spatial analysis focuses on PM_{2.5} peaks during the early hours of January 1, 2024, from
291 00:00 and up to 07:00 (GMT-6). During this timeframe, EMGA sensors observed a notable
292 increase in PM_{2.5} recordings, some of them up to 1000% higher than the usual values on the
293 same hours. For the analysis, the maximum mean values from each of the 11 stations utilized
294 in this study were considered (Figure 8). Data analyzed correspond to the period from
295 December 10, 2023, to January 10, 2024. Outlier data were excluded by filtering to calculate
296 the averages, as mentioned in Sect. 2.2. Figure 8a displays the maximum values recorded for
297 February 12, 2024 (Monday), considered a random typical day of activity in the city. Figure
298 8b illustrates the spatial distribution of PM_{2.5} records, highlighting the highest readings
299 observed at STATION-10, located in the central area of the city. This region is recognized as
300 one of the most densely populated areas in the city and is adjacent to two significant industrial
301 zones. Additionally, it is characterized by nearby neighborhoods where various regional and
302 local festivities, such as religious festivals, occur more frequently than in other parts of the
303 city. Conversely, the lowest readings correspond to STATION-13, located in the southwest
304 area of the city. This site is positioned between the Bernardo Quintana Industrial Park and
305 the Cimatario National Park ecological reserve and boasts one of the lowest population
306 densities in the city. Despite experiencing intense activity on regular working days and hours,
307 human activity, including both traffic and industrial activities, is notably diminished during
308 the early hours of January 1, compared to other parts of the city, resulting in the lowest PM_{2.5}
309 recordings among all stations during that period. Table 1 presents the maximum PM_{2.5}
310 concentration values recorded by the stations for January 1 and February 12.

311

312

313 *3.7 Infrasound data*

314

315 In addition to analyzing particulate matter concentrations, an examination of infrasound data
316 was conducted to identify trends associated with the burning of pyrotechnics. For this
317 purpose, data from an infrasound station installed at the same location as station STATION-
318 10 were analyzed from December 19, 2023, to January 6, 2024. Figure 9a displays the time
319 series of the normalized data, where no significant difference is observed for January 1. To
320 discern specific trends, a seasonal trend decomposition (STL) analysis was employed. This
321 statistical technique separates the trend, seasonality, and noise components of a given time
322 series dataset (Shumway, 2017; Hyndman, 2018). Figure 9b presents the graph generated
323 with the trend adjustment obtained by STL, indicating a trend towards an increase in activity
324 during the late hours of December 31, 2023, continuing into the early hours of January 1,
325 2024, before normalizing for the rest of the day. This trend aligns with observations in PM_{2.5}
326 records from EMGA stations during the same timeframe. Figure 9c compares the original
327 normalized time series with the STL trend data, highlighting the noticeable trend towards
328 increased activity, which can be associated with the rise in pyrotechnic burning.

329

330

331 **4. Discussion**

332

333 The use of low-cost sensors presents a feasible and economical alternative for monitoring air
334 quality in urban settings exposed to various sources of pollution. While these sensors may
335 not offer the same level of precision as reference equipment, they serve as valuable tools for

336 identifying the sources and dispersion of contaminants stemming from human activities, as
337 well as their correlation with climatic variables like temperature, humidity and other climate
338 conditions (Badura, 2018; Tryner et al., 2020; Nguyen et al., 2021; Karaoghlanian et al.,
339 2022; Jaffe et al., 2023). The data presented in this study highlight contamination sources
340 from burning pyrotechnics, occurring over several hours and distributed across the city.

341

342 Real-time recordings provided by sensors enable the observation of varying environmental
343 conditions (deterioration of air quality), including changes in particulate matter
344 concentration. Short-term fluctuations, spanning from minutes to hours, are frequently linked
345 to human activity, which can exert significant short- and medium-term impacts on the
346 environment. In this study, we analyze the substantial increase in atmospheric $PM_{2.5}$
347 concentration resulting from fireworks burning. Spatially, Figure 4b illustrates station
348 distribution and their peak values recorded during the early hours of January 1, 2024,
349 showing considerable increases across most stations compared to typical values depicted in
350 Figure 4a. The spatial distribution identifies areas where fireworks burning was more intense
351 during that period, associating it as a source of contamination during short-term events.

352

353 Complementing spatial distribution, time series analysis reveals $PM_{2.5}$ concentration
354 variations over time. A significant increase is observed in $PM_{2.5}$ concentrations recorded on
355 December 25 and January 1 across most stations, indicating a substantial rise in atmospheric
356 pollutants generated within a few hours due to fireworks burning. Each station's location
357 reflects changes corresponding to predominant human activity in its area. For instance,
358 STATION-13, situated in an industrial area, exhibits no significant increase in $PM_{2.5}$
359 concentrations during the indicated dates, suggesting lower human activity compared to

360 residential areas like stations 10 and 19. This underscores the anthropogenic influence on
361 $PM_{2.5}$ concentration during short-duration events.

362

363 Weekly and hourly trends display a consistent pattern aligned with human activity, with $PM_{2.5}$
364 concentration fluctuations marked by peak times of anthropogenic activity such as vehicular
365 traffic and industrial operations. However, as depicted in Figures 7a, 7b, 8a, and 8b,
366 pyrotechnic activity disrupts these trends, substantially elevating $PM_{2.5}$ concentrations
367 compared to periods of lower activity.

368

369 Real-time monitoring proves crucial, allowing for the recording and characterization of short-
370 lived events in time and space. Despite their brief duration, such events significantly impact
371 environmental conditions, potentially affecting human health and urban fauna diversity.
372 Figure 8 demonstrates how high $PM_{2.5}$ concentrations may go statistically unnoticed in
373 longer-term records, with only more frequent concentrations observed in the normal
374 distribution. This fact underscores the challenge of quantifying and associating short-term
375 effects with other anthropogenic and environmental issues, such as forest fires, waste burning
376 outdoors, accidental fires, and barbecues, among others.

377

378 Furthermore, analyzing $PM_{2.5}$ data in conjunction with other parameters, such as infrasound
379 (Figure 9), can reveal trends indicating pollution increases associated with anthropogenic
380 activity, as recorded by other monitoring devices like seismic or geomagnetic stations.

381

382 The bursting and burning of firecrackers during festivities can cause significant damage to
383 human health every year. Consumer firework-related physical injuries can be devastating,

384 leading to permanent vision loss, limb amputations, and, in some cases, death (Puri et al.,
385 2009; Tandom et al., 2012; Turgut et al., 2022). On the other hand, exposure to PM_{2.5} can
386 cause acute and chronic health problems, as evidence shows that exposure to the particulate
387 is linked to cardiovascular disorders such as heart attacks, heart failure, arrhythmias, and
388 strokes (Krittanawong et al., 2023; Garcia et al., 2023). More critical are the respiratory
389 effects, such as asthma attacks and exacerbated respiratory symptoms like sneezing,
390 wheezing, and shortness of breath, as exposure to PM_{2.5} is associated with those respiratory
391 disorders (Ren et al., 2017; Cao et al., 2018; Garcia et al., 2023). As a general diagnosis of
392 the air quality situation in Queretaro during New Year's Eve, it can be said that the urban area
393 presents a spike of PM_{2.5} values that can cause an increase of cardiovascular risk factors but
394 especially a high number of cases of respiratory disorder.

395

396 In the case of pets and urban fauna, health issues manifest as cardiopulmonary problems,
397 alongside visual and auditory overstimulation that disrupts behavior. Elevated concentrations
398 of PM_{2.5} and PM₁₀ particles impact airway epithelial cells and vascular endothelial cells,
399 resulting in lung inflammation within the initial 24-hour period post-inhalation. Research
400 conducted in laboratories has shown that PM_{2.5} particles exert a more pronounced effect on
401 mammalian health, escalating the production of reactive oxygen species (Hickey et al., 2020).
402 While these molecules typically play roles in cellular functions, heightened levels can induce
403 oxidative stress, causing potential damage to cellular structures or genetic material. The
404 sudden loud noises and intense brightness of fireworks trigger fear and confusion among
405 animals. Pet dogs often display signs of fear, particularly in response to noise, such as
406 heightened activity, panting, vocalizations, blinking, and seeking out hiding spots (Gähwiler

407 et al., 2020). It's worth noting that not all individuals respond identically to stress, which may
408 explain why some do not exhibit obvious signs of fear (Gähwiler et al., 2020).

409

410 Regarding urban fauna, birds are sensitive to loud noises and intense light (Shamoun-Baranes
411 et al., 2011; Hoekstra et al., 2024). Observations suggest that in open fields or agricultural
412 areas, birds seek shelter and gather in large numbers (Shamoun-Baranes et al., 2011; Hoekstra
413 et al., 2024). In Querétaro, where the highest pyrotechnic activity is recorded, the site is
414 adjacent to open fields, indicating that birds, mammals, and other organisms such as insects
415 will react and congregate in this area (Shamoun-Baranes et al., 2011; Hoekstra et al., 2024;
416 see Figure 10). Although there is insufficient information regarding the effects on insects and
417 other invertebrates, it is presumed that similar to vertebrates, inhaled particles affect their
418 respiratory system, while loud noises, shock waves, and light impact their auditory system,
419 leading to confusion due to their positive phototropism. This latter point is closely linked to
420 their transversal orientation system, utilized by different organisms such as moths to navigate
421 their environment with the Moon as a reference point (Warrant & Dacke, 2010).

422

423 **5. Conclusions**

424

425 The recording of environmental pollution through the use of low-cost sensors provides
426 valuable data for monitoring human activity. Particularly this study highlights short-term
427 events such as fireworks burning. These brief events may go unnoticed in long-term time
428 series. Additionally, the importance of low-cost environmental monitoring networks is
429 demonstrated, providing data over long periods and enabling spatial analysis, thereby
430 inferring anthropogenic impacts on environmental conditions. In this study, it was shown

431 how two events lasting approximately 10 hours resulted in particulate matter concentrations
432 up to 10 times higher than on a regular day. This could have negative consequences for human
433 health and urban fauna diversity. Analyzing these events can facilitate the design of
434 mitigation measures to reduce environmental damage.

435

436

437 **Acknowledgements**

438 This work was supported by project IG-101921. Dr. Rodríguez-Trejo acknowledged the
439 support from CONAHCYT for the postdoctoral fellowship EPM 2022 (2). Special thanks to
440 J. Escalante-González for the technical support.

441

442 *Data availability*

443 Data available on demand.

444

445 *Funding*

446 This work was funded by: UNAM-DGAPA PAPITT IG-101921

447

448 *Statement*

449 Alejandro Rodríguez-Trejo: conceptualization, writing, interpretation, figures, technical
450 development and programming of the device and the visualization platform; Héctor Enrique
451 Ibarra-Ortega: technical development of the equipment, reviewing; Harald Böhnel:
452 Conceptualization, reviewing, technical development of the device; Reneé González-
453 Guzmán: writing, interpretation, reviewing, figures; Luis Enrique Sánchez-Ramos: writing,
454 interpretation, reviewing, figures; Ana Gabriela Castañeda-Miranda: writing, interpretation,

455 reviewing; Víctor Hugo Márquez Ramírez: infrasound data acquisition, reviewing; Marcos
456 Adrián Eduardo Chaparro: writing, interpretation, reviewing; Mauro Alejandro Eduardo
457 Chaparro: writing, interpretation, reviewing.

458

459 *Competing interest declaration*

460

461 The authors declare that there is no competing interest in the present work.

462

463

464

465 **References**

466 Ambade, B. (2018). The air pollution during Diwali festival by the burning of
467 fireworks in Jamshedpur city, India. *Urban climate*, 26, 149-160.

468

469 Ardon-Dryer, K., Dryer, Y., Williams, J. N., & Moghimi, N. (2020). Measurements
470 of PM_{2.5} with PurpleAir under atmospheric conditions. *Atmospheric Measurement*
471 *Techniques*, 13(10), 5441-5458.

472

473 Badura, M., Batog, P., Drzeniecka-Osiadacz, A., & Modzel, P. (2018). Evaluation of
474 low-cost sensors for ambient PM_{2.5} monitoring. *Journal of Sensors*, 2018.

475

476 Barkjohn, K. K., Gantt, B., & Clements, A. L. (2020). Development and
477 Application of a United States wide correction for PM_{2.5} data collected with the
478 PurpleAir sensor. *Atmospheric Measurement Techniques Discussions*, 2020, 1-34.

479

480 Camprodon, G., González, Ó., Barberán, V., Pérez, M., Smári, V., de Heras, M. Á., &
481 Bizzotto, A. (2019). Smart Citizen Kit and Station: An open environmental monitoring
482 system for citizen participation and scientific experimentation. *HardwareX*, 6, e00070.

483

484 Cao, Q., Rui, G., & Liang, Y. (2018). Study on PM_{2.5} pollution and the mortality
485 due to lung cancer in China based on geographic weighted regression model. *BMC public*
486 *health*, 18, 1-10.

487

488 Castañeda-Miranda, A.G., Chaparro, M.A.E., Pacheco-Castro, A., Chaparro, M.A.E.,
489 Böhnelt, H.N., 2020. Magnetic biomonitoring of atmospheric dust using tree leaves of *Ficus*
490 *benjamina* in Queretaro (Mexico). *Environ. Monit. Assess.* [https://doi.org/10.1007/s10661-](https://doi.org/10.1007/s10661-020-8238-x)
491 [020-8238-x](https://doi.org/10.1007/s10661-020-8238-x).

492 Chaparro, M.A.E.; Buitrago Posada, D.; Chaparro, M.A.E.; Molinari, D.; Chiavarino,
493 L.; Alba, B.; Marié, D.C.; Natal, M.; Böhnelt, H.N.; Vaira, M., 2024. Urban and suburban's
494 airborne magnetic particles accumulated on *Tillandsia capillaris*. *Sci. Total Environ.* 907,
495 167890. <https://doi.org/10.1016/j.scitotenv.2023.167890>

496

497 Chen, L., Pang, X., Li, J., Xing, B., An, T., Yuan, K., ... & Chen, J. (2022). Vertical
498 profiles of O₃, NO₂ and PM in a major fine chemical industry park in the Yangtze River
499 Delta of China detected by a sensor package on an unmanned aerial vehicle. *Science of the*
500 *Total Environment*, 845, 157113.

501

502 Chhabra, A., Turakhia, T., Sharma, S., Saha, S., Iyer, R., & Chauhan, P. (2020).
503 Environmental impacts of fireworks on aerosol characteristics and radiative properties over
504 a mega city, India. *City and Environment interactions*, 7, 100049.

505

506 Farooqui, Z.; Biswas, J.; Saha, J. Long-Term Assessment of PurpleAir Low-Cost
507 Sensor for PM_{2.5} in California, USA. *Pollutants* **2023**, 3, 477–493.
508 <https://doi.org/10.3390/pollutants3040033>

509

510 Feng, B., Li, L., Xu, H., Wang, T., Wu, R., Chen, J., ... & Huang, W. (2019). PM_{2.5}-
511 bound polycyclic aromatic hydrocarbons (PAHs) in Beijing: Seasonal variations, sources,
512 and risk assessment. *Journal of Environmental Sciences*, 77, 11-19.

513

514 Gähwiler, S., Bremhorst, A., Tóth, K., & Riemer, S. (2020). Fear expressions of dogs
515 during New Year fireworks: a video analysis. *Scientific reports*, 10(1), 16035.

516

517 Garcia, A., Santa-Helena, E., De Falco, A., de Paula Ribeiro, J., Gioda, A., & Gioda,
518 C. R. (2023). Toxicological effects of fine particulate matter (PM_{2.5}): health risks and
519 associated systemic injuries—systematic review. *Water, Air, & Soil Pollution*, 234(6), 346.

520

521 Giordano, M. R., Malings, C., Pandis, S. N., Presto, A. A., McNeill, V. F., Westervelt,
522 D. M., ... & Subramanian, R. (2021). From low-cost sensors to high-quality data: A summary

523 of challenges and best practices for effectively calibrating low-cost particulate matter mass
524 sensors. *Journal of Aerosol Science*, 158, 105833.

525

526 Gouder, C., & Montefort, S. (2014). Potential impact of fireworks on respiratory
527 health. *Lung India*, 31(4), 375-379.

528

529 Hickey, C., Gordon, C., Galdanes, K., Blaustein, M., Horton, L., Chillrud, S., Ross,
530 J., Yinon, L., Chen, L. C., & Gordon, T. (2020). Toxicity of particles emitted by fireworks.
531 *Particle and fibre toxicology*, 17, 1-11.

532

533 Hoekstra, B., Bouten, W., Dokter, A., van Gasteren, H., van Turnhout, C.,
534 Kranstauber, B., van Loon, E., Leijnse, H., & Shamoun-Baranes, J. (2024). Fireworks
535 disturbance across bird communities. *Frontiers in Ecology and the Environment*, 22(1),
536 e2694.

537

538 Hyndman, R. J., & Athanasopoulos, G. (2018). *Forecasting: Principles and Practice*.
539 OTexts.

540

541 Instituto Nacional de Estadística y Geografía (INEGI). 2020. Censo de población y
542 vivienda 2020. México: Instituto Nacional de Estadística y Geografía.
543 <https://www.inegi.org.mx/programas/ccpv/2020/>

544

545

546 Jaffe, D. A., Thompson, K., Finley, B., Nelson, M., Ouimette, J., & Andrews, E.
547 (2023). An evaluation of the US EPA's correction equation for PurpleAir sensor data in
548 smoke, dust, and wintertime urban pollution events. *Atmospheric Measurement Techniques*,
549 *16*(5), 1311-1322.

550

551 Jiao, W., Hagler, G., Williams, R., Sharpe, R., Brown, R., Garver, D., Judge, R., &
552 Caudill, M. (2015). Community Air Sensor Network (CAIRSENSE) project: evaluation of
553 low-cost sensor performance in a suburban environment in the southeastern United States.
554 *Atmospheric Measurement Techniques*, *8*(4), 1443-1460.

555

556 Karaoghlanian, N., Nouredine, B., Saliba, N., Shihadeh, A., & Lakkis, I. (2022). Low
557 cost air quality sensors "PurpleAir" calibration and inter-calibration dataset in the context
558 of Beirut, Lebanon. *Data in Brief*, *41*.

559

560

561 Kaur, K., & Kelly, K. E. (2023). Laboratory evaluation of the Alphasense OPC-N3,
562 and the Plantower PM2.5S5003 and PM2.5S6003 sensors. *Journal of Aerosol Science*, *171*,
563 106181.

564

565 Krittanawong, C., Qadeer, Y. K., Hayes, R. B., Wang, Z., Thurston, G. D., Virani, S.,
566 & Lavie, C. J. (2023). PM_{2.5} and cardiovascular diseases: State-of-the-Art review.
567 *International Journal of Cardiology Cardiovascular Risk and Prevention*, 200217.

568

569 Kuula, J., Mäkelä, T., Aurela, M., Teinilä, K., Varjonen, S., González, Ó., & Timonen,
570 H. (2020). Laboratory evaluation of particle-size selectivity of optical low-cost particulate
571 matter sensors. *Atmospheric Measurement Techniques*, 13(5), 2413-2423.

572

573 Li YouPing, L. Y., Zhang ZhiSheng, Z. Z., Liu HuiFang, L. H., Zhou Hong, Z. H.,
574 Fan ZhongYu, F. Z., Lin Mang, L. M., ... & Xia BeiCheng, X. B. (2016). Characteristics,
575 sources and health risk assessment of toxic heavy metals in PM_{2.5} at a megacity of southwest
576 China. *Environmental geochemistry and health*, 2016, vol. 38, p. 353-362.

577

578 Lin, C. C. (2016). A review of the impact of fireworks on particulate matter in ambient
579 air. *Journal of the Air & Waste Management Association*, 66(12), 1171-1182.

580

581 McIntosh, G.; Gómez-Paccard, M.; Osete, M.L. (2007). The Magnetic Properties of
582 Particles Deposited on *Platanus x hispanica* Leaves in Madrid, Spain, and their Temporal and
583 Spatial Variations. *Sci. Total Environ.*, 382, 135–146

584

585 Mousavi, A., Yuan, Y., Masri, S., Barta, G., & Wu, J. (2021). Impact of 4th of July
586 fireworks on spatiotemporal PM_{2.5} concentrations in California based on the PurpleAir
587 Sensor Network: Implications for policy and environmental justice. *International journal of*
588 *environmental research and public health*, 18(11), 5735.

589

590 Nguyen, N. H., Nguyen, H. X., Le, T. T., & Vu, C. D. (2021). Evaluating low-cost
591 commercially available sensors for air quality monitoring and application of sensor
592 calibration methods for improving accuracy.

593

594 Paoli, L., Winkler, A., Guttova, A., Sagnotti, A., Grassi, A., Lackovicova, A., Senko,
595 D., Loppi, S., 2017. Magnetic properties and element concentrations in lichens exposed to
596 airborne pollutants released during cement production. *Environ. Sci. Pollut. Res.* 24 (13),
597 12063–12080. <https://doi.org/10.1007/s11356-016-6203-6>.

598

599 Puri, V., Mahendru, S., Rana, R. and Deshpande, M., 2009. Firework injuries: a ten-
600 year study. *Journal of Plastic, Reconstructive & Aesthetic Surgery*, 62(9), pp.1103-1111.

601

602 Ren, M., Fang, X., Li, M., Sun, S., Pei, L., Xu, Q., ... & Cao, Y. (2017). Concentration-
603 Response Relationship between PM 2.5 and Daily Respiratory Deaths in China: A Systematic
604 Review and Metaregression Analysis of Time-Series Studies. *BioMed research international*,
605 2017.

606

607 Rossol, M. "Arts, Crafts, Theater, and Entertainment." (2014): 317-322.

608

609 Searle, N., Kaur, K., & Kelly, K. (2023). Identifying a performance change in the
610 Plantower PM2.5S 5003 particulate matter sensor. *Journal of Aerosol Science*, 174, 106256.

611

612 Shamoun-Baranes, J., Dokter, A. M., van Gasteren, H., van Loon, E. E., Leijnse, H.,
613 & Bouten, W. (2011). Birds flee en mass from New Year's Eve fireworks. *Behavioral*
614 *Ecology*, 22(6), 1173-1177.

615

616 Shumway, R. H., & Stoffer, D. S. (2017). *Time Series Analysis and Its Applications:*
617 *With R Examples*. Springer.

618

619 Sousan, S., Koehler, K., Hallett, L., & Peters, T. M. (2016). Evaluation of the
620 Alphasense Optical Particle Counter (OPC-N2) and the Grimm Portable Aerosol
621 Spectrometer (PAS-1.108). *Aerosol Science and Technology*, 50(2), 135-144.

622

623 Stavroulas, I., Grivas, G., Michalopoulos, P., Liakakou, E., Bougiatioti, A.,
624 Kalkavouras, P., ... & Gerasopoulos, E. (2020). Field evaluation of low-cost PM2.5 sensors
625 (Purple Air PA-II) under variable urban air quality conditions, in Greece. *Atmosphere*, 11(9),
626 926.

627

628 Tandon, R., Agrawal, K., Narayan, R. P., Tiwari, V. K., Prakash, V., Kumar, S., &
629 Sharma, S. (2012). Firecracker injuries during Diwali festival: The epidemiology and impact
630 of legislation in Delhi. *Indian journal of plastic surgery*, 45(01), 097-101.

631

632 Tryner, J., L'Orange, C., Mehaffy, J., Miller-Lionberg, D., Hofstetter, J. C., Wilson,
633 A., & Volckens, J. (2020). Laboratory evaluation of low-cost PurpleAir PM monitors and in-

634 field correction using co-located portable filter samplers. *Atmospheric Environment*, 220,
635 117067.

636

637 Turgut, Ferhat, Alexandra Bograd, Brida Jeltsch, Adrian Weber, Petra Schwarzer,
638 Iulia M. Ciotu, Joao Amaral et al. "Occurrence and outcome of firework-related ocular
639 injuries in Switzerland: a descriptive retrospective study." *BMC ophthalmology* 22, no. 1
640 (2022): 296.

641

642 Warrant, E., & Dacke, M. (2010). Visual orientation and navigation in nocturnal
643 arthropods. *Brain Behavior and Evolution*, 75(3), 156-173.

644

645 *Table*

646

647

	January 01, 2024	February 12, 2024
Station Name	Max PM _{2.5} (µg/m ³)	
<i>STATION-19</i>	160	28
<i>STATION-12</i>	265	50
<i>STATION-10</i>	346	42
<i>STATION-11</i>	267	52
<i>STATION-18</i>	178	43
<i>STATION-13</i>	56	39
<i>STATION-01</i>	198	51

<i>STATION-03</i>	112	34
<i>STATION-17</i>	231	26
<i>STATION-07</i>	274	53
<i>STATION-22</i>	255	58

648

649 Table 1. Maximum PM_{2.5} concentrations recorded at monitoring stations for January 1st and
650 February 12th, 2024, illustrate the significant difference between recordings on two different
651 days.

652

653 *Captions*

654

655 Figure. 1 Location of Querétaro city compared to other cities in central Mexico (left). The
656 spatial location of the EMGA stations from the environmental monitoring network of
657 Querétaro city (right).

658

659 Figure. 2 Time series showing increases in PM_{2.5} concentrations at three monitoring stations.
660 (a) Displays the values recorded at STATION-10; (b) The values recorded by STATION-19;
661 (c) Shows the recordings from STATION-13.

662

663 Figure 3. Comparison among three time-series showing increases in PM_{2.5} concentrations at
664 three monitoring stations. Series 1 (red) displays the values recorded at STATION-10; series
665 2 (blue) shows the values recorded by STATION-13; and series 3 (green) depicts the
666 recordings from STATION-19.

667

668 Figure 4. Comparison with temperature (up) and humidity (down) dependence of the PM_{2.5}
669 concentration.

670

671 Figure 5. Trends by day of the week from Monday to Sunday, and by hour of the day. The
672 graph illustrates the hourly and daily trend of PM_{2.5} concentration during the study period.

673

674 Figure 6. Polar representation showing trends of PM_{2.5} concentration in hourly averages.
675 Each color indicates hourly averages for a full day of data.

676

677 Figure 7. Histograms of PM_{2.5} concentrations grouped into 5 $\mu\text{g}/\text{m}^3$ ranges and fitting to a
678 normal distribution.

679

680 Figure 8 Spatial distribution of maximum PM_{2.5} concentrations recorded in the monitoring
681 network for February 12th, 2024 (a); and for January 1st, 2024 (b). The inset (below) displays
682 the ranges of PM_{2.5} concentrations in $\mu\text{g}/\text{m}^3$.

683

684 Figure 9. Infrasond data recorded at STATION-10 between December 29th, 2023, and
685 January 6th, 2024. (a) Shows the time series plot of normalized data; (b) Trend plot of the
686 Seasonal Decomposition of Time Series (STL) applied to the time series; (c) Comparison
687 between the trend plots and the infrasond time series.

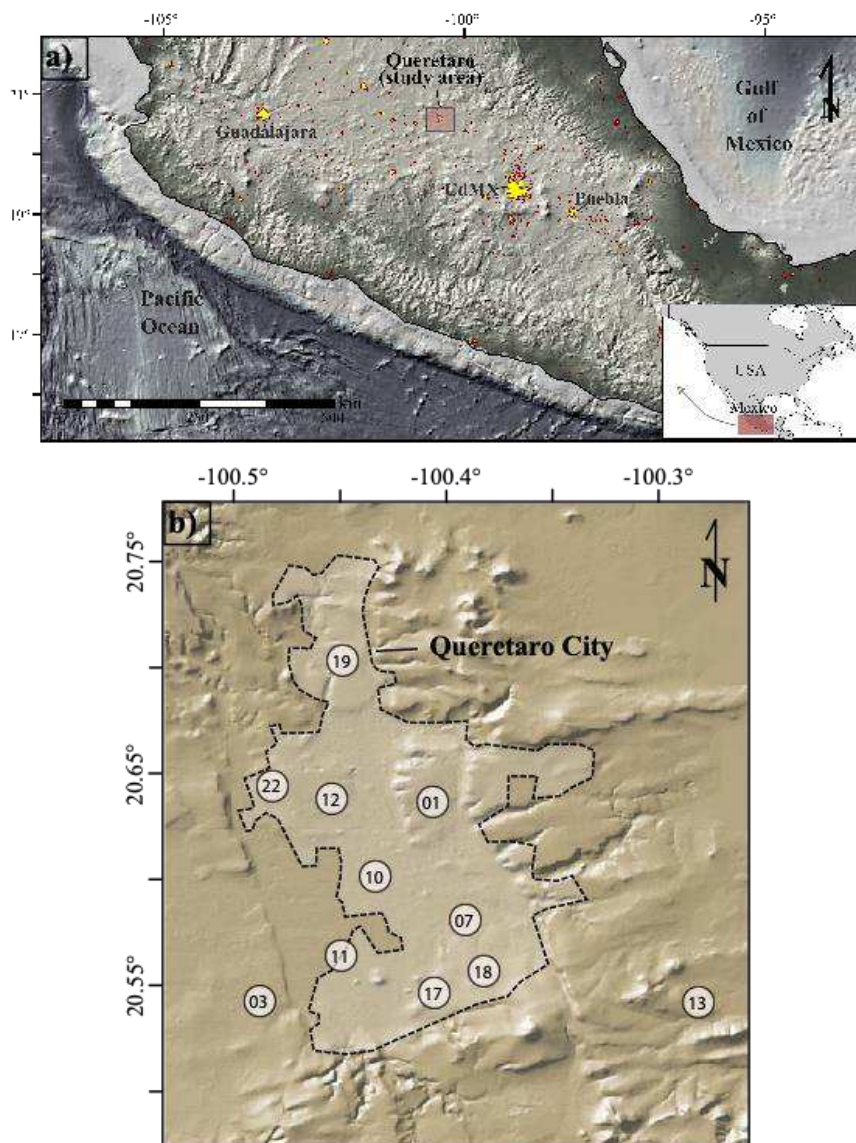
688

689 Figure 10. Areas within the city of Querétaro where records of insects and birds have been
690 documented. The red heat points represent the locations of EMGAs (Ecological Monitoring

691 and Management Areas) and their corresponding maximum values. Lighter shades of red
692 indicate lower values, while darker shades indicate higher values. GBIF Occurrence
693 Download <https://doi.org/10.15468/dl.emurnt>.

694

695 *Figures*



696

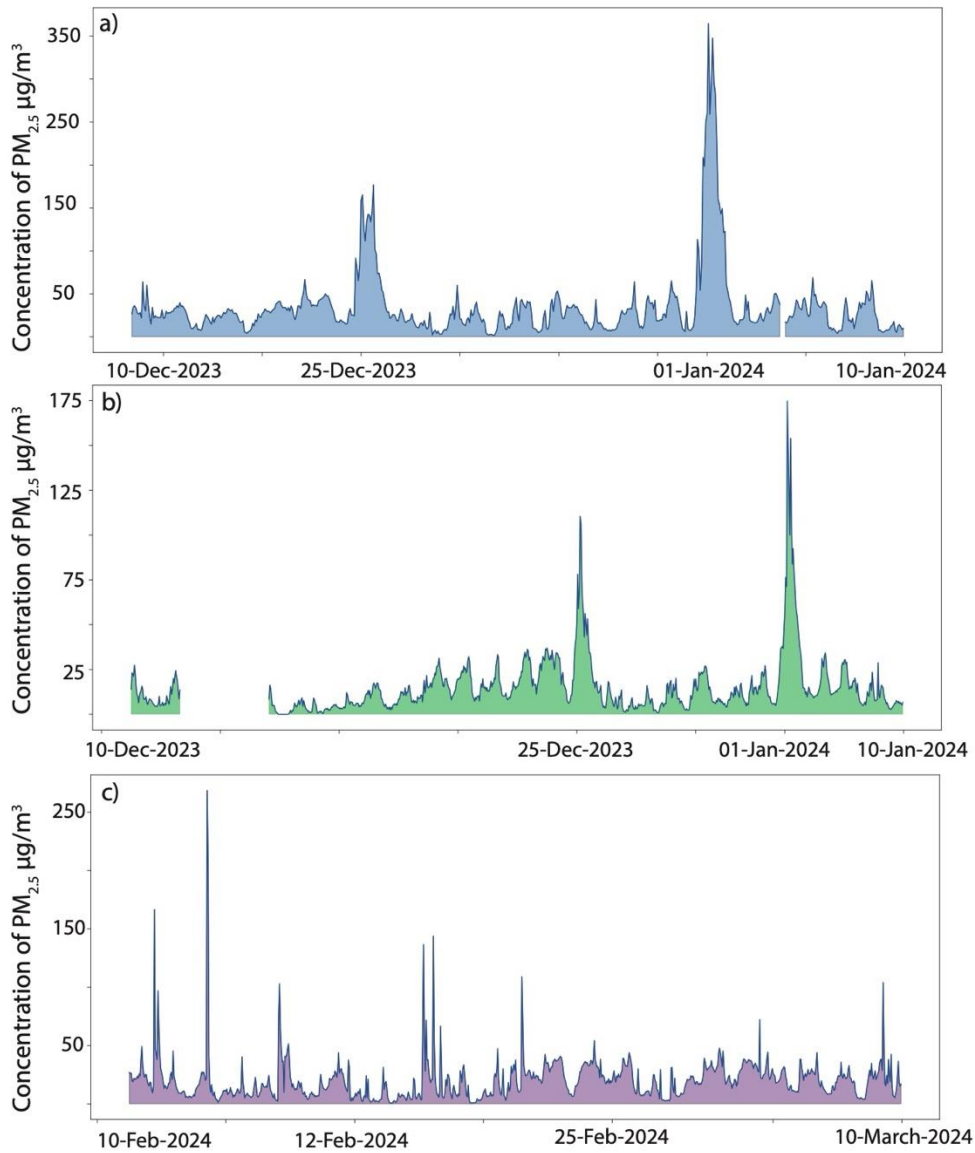
697 Figure 1

698

699

700

701



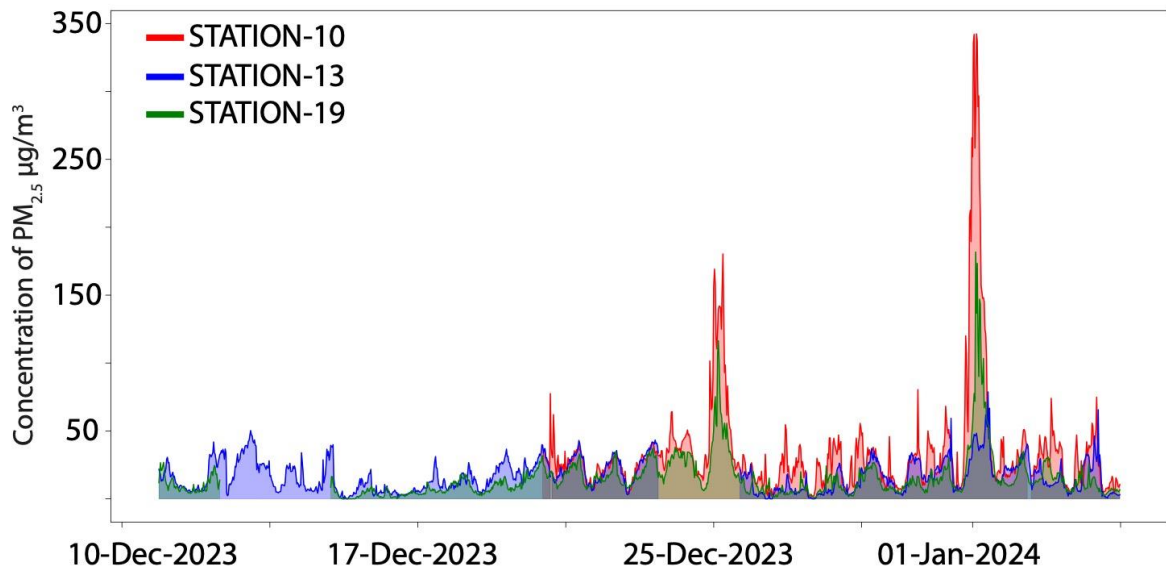
702

703 Figure. 2

704

705

706
707
708
709
710
711
712
713
714
715



716
717
718
719
720
721

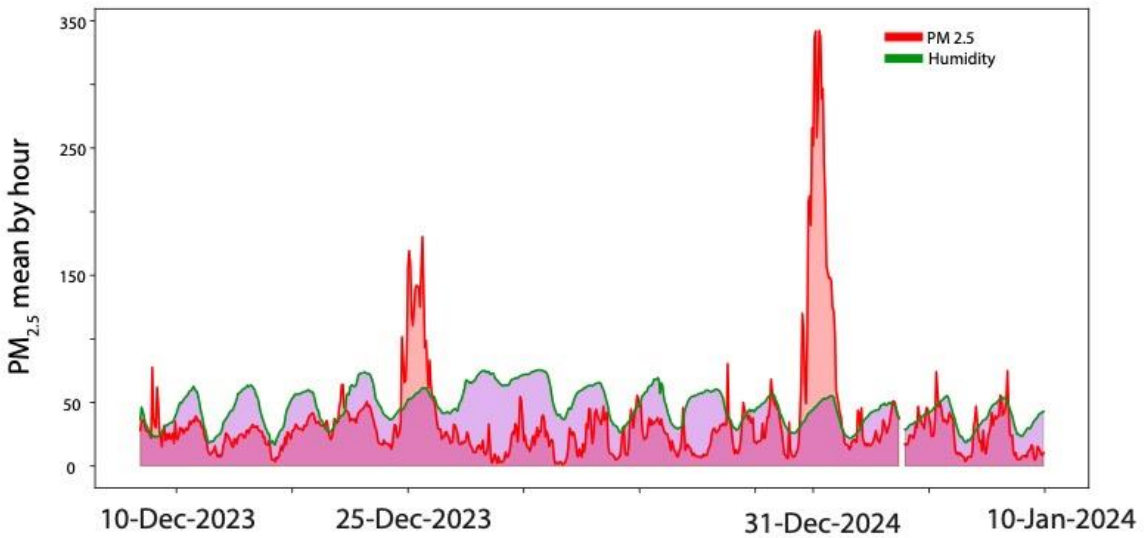
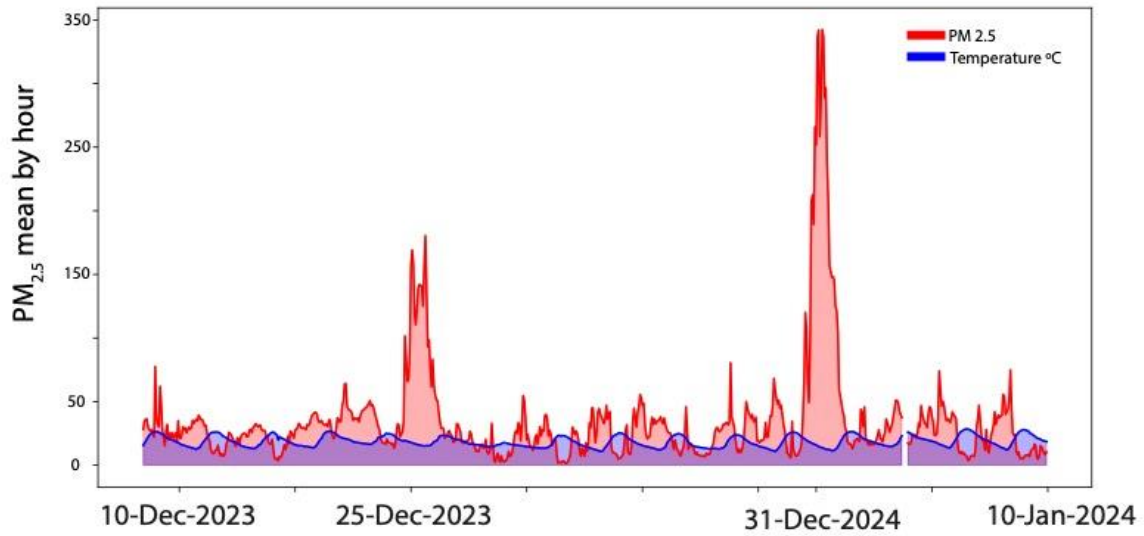
Figure. 3

722

723

724

725



726

727 Figure. 4.

728

729

730

731

732

733

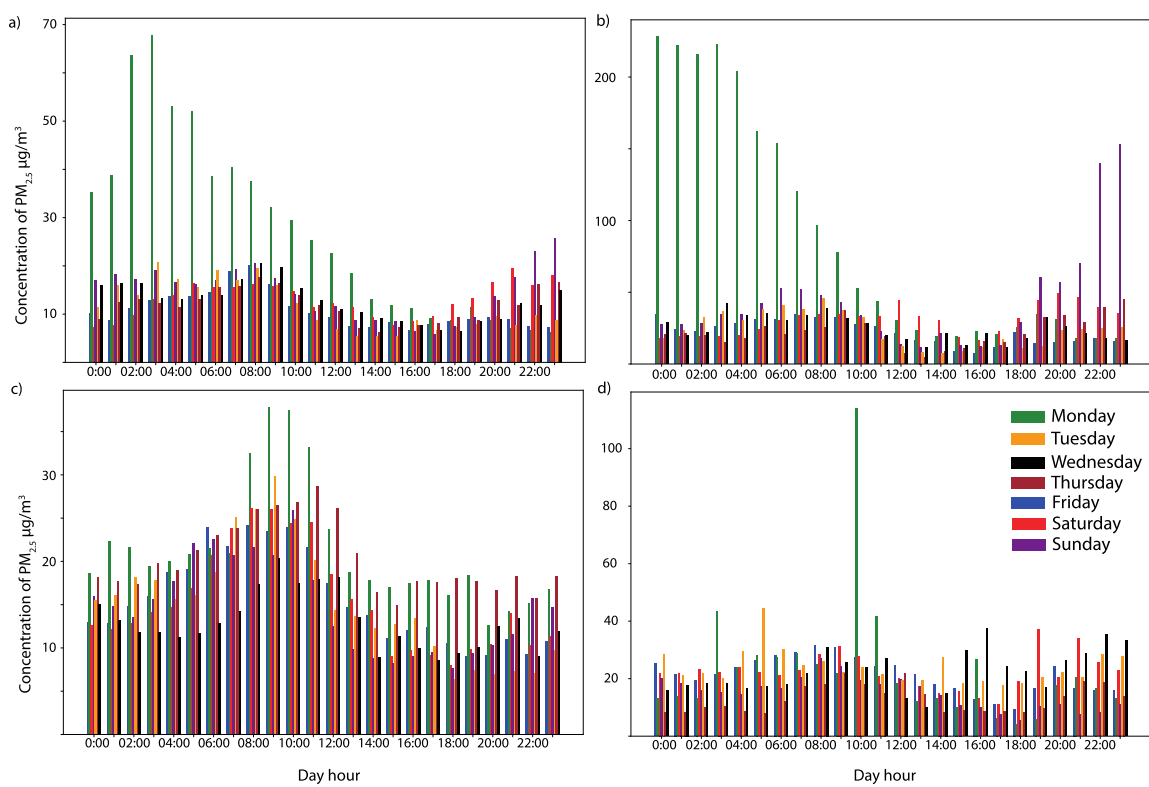
734

735

736

737

738



739

740 Figure. 5

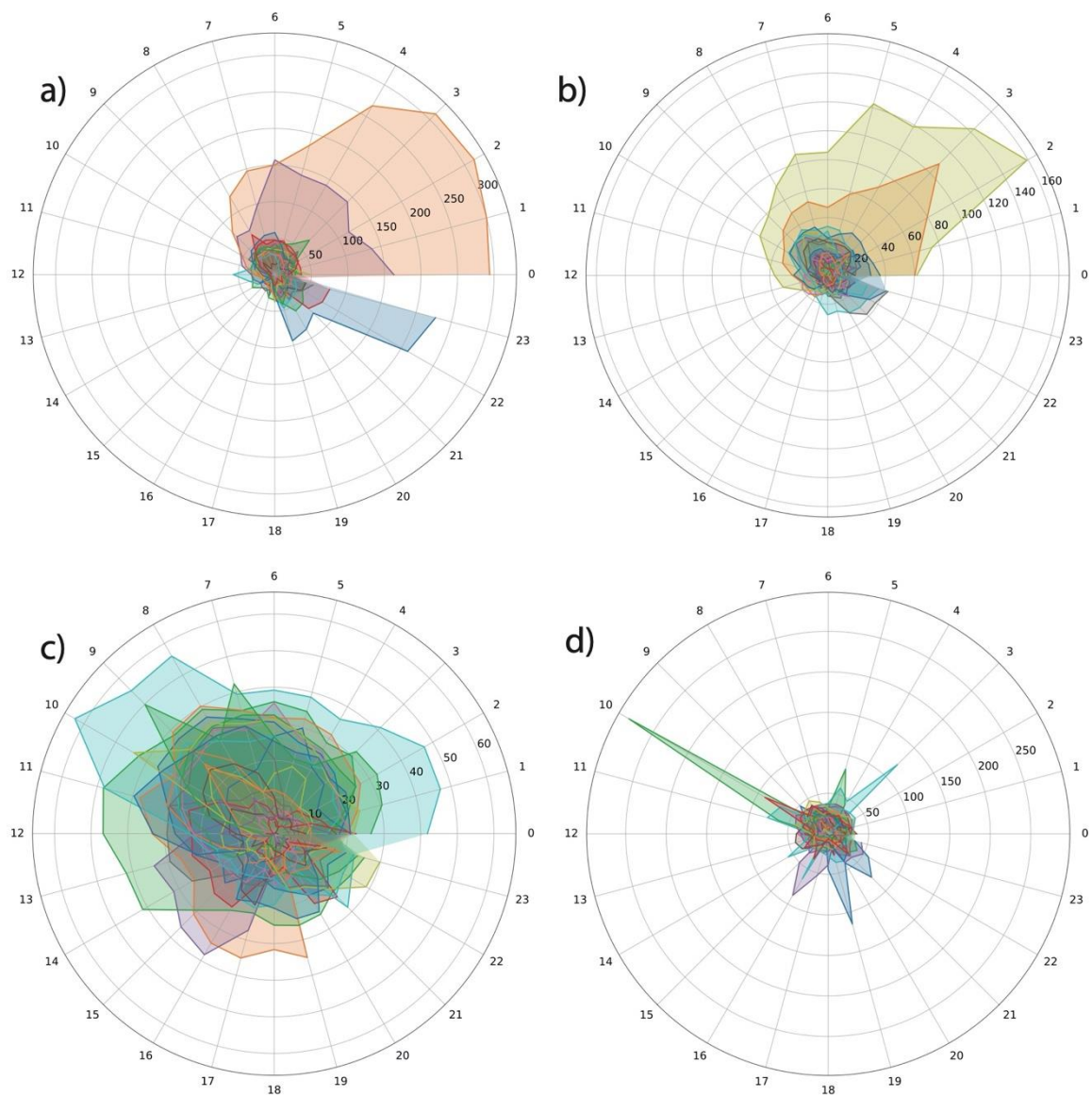
741

742

743

744

745



746

747 Figure. 6

748

749

750

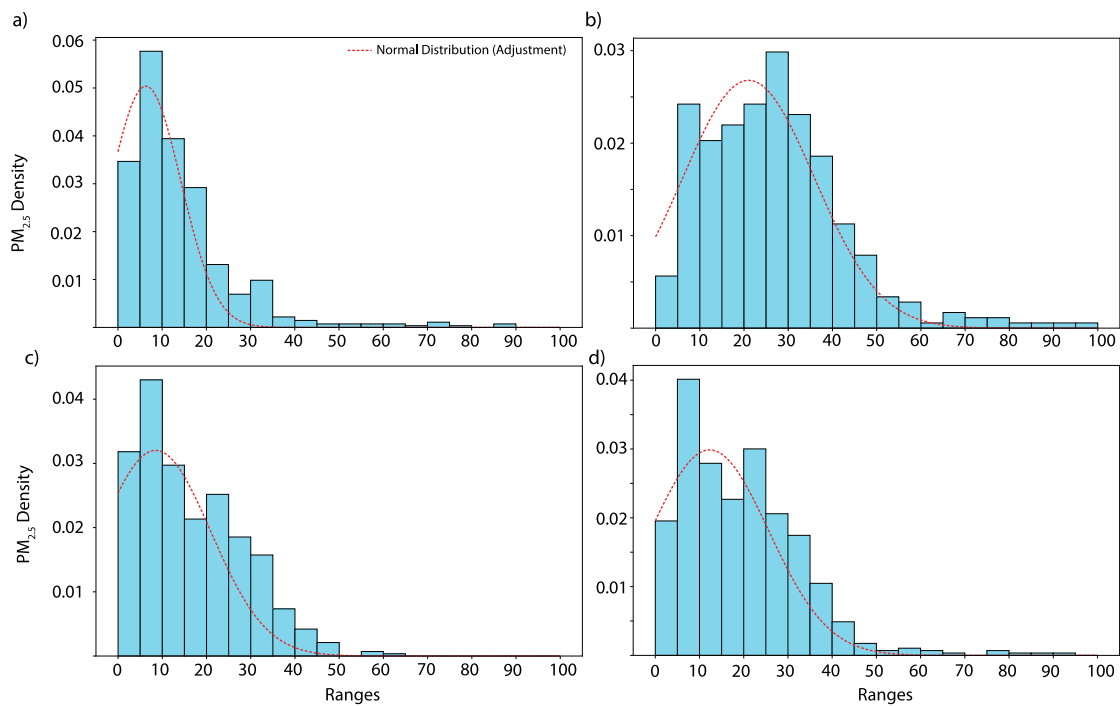
751

752

753

754

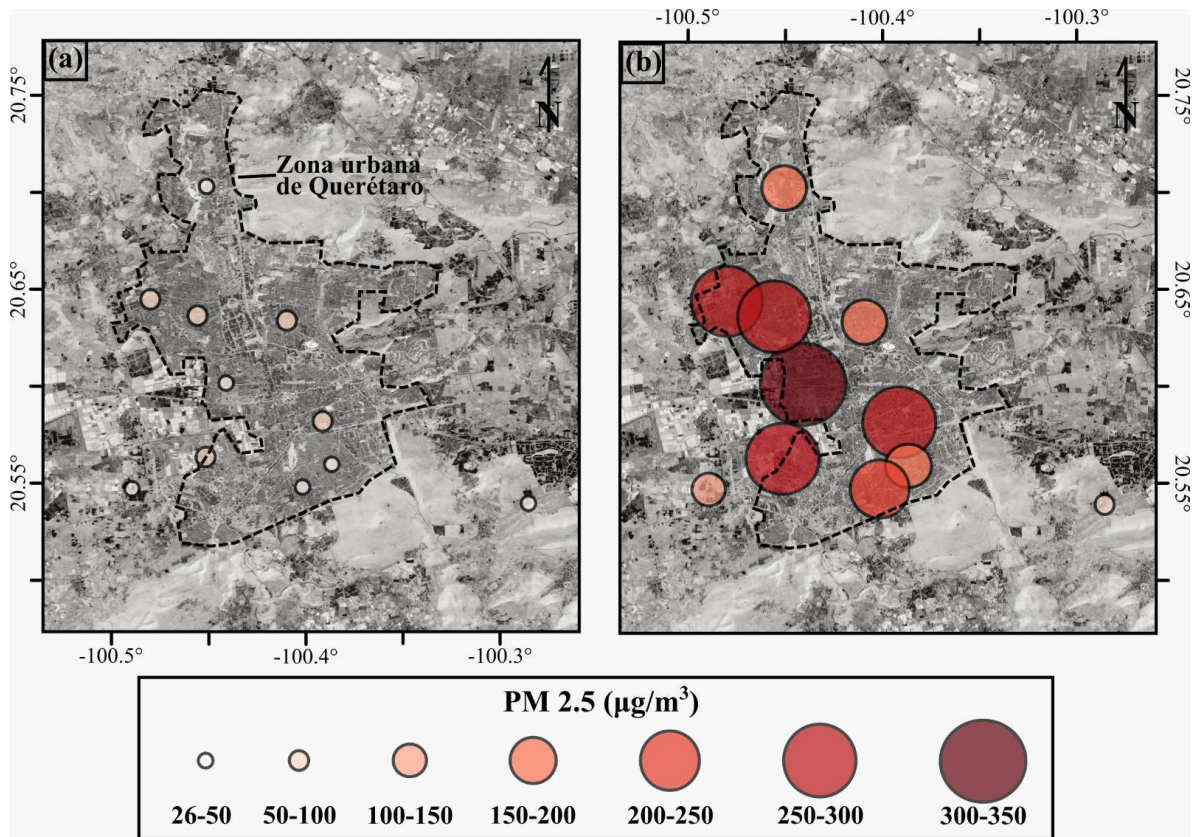
755



756

757 Figure 7

758



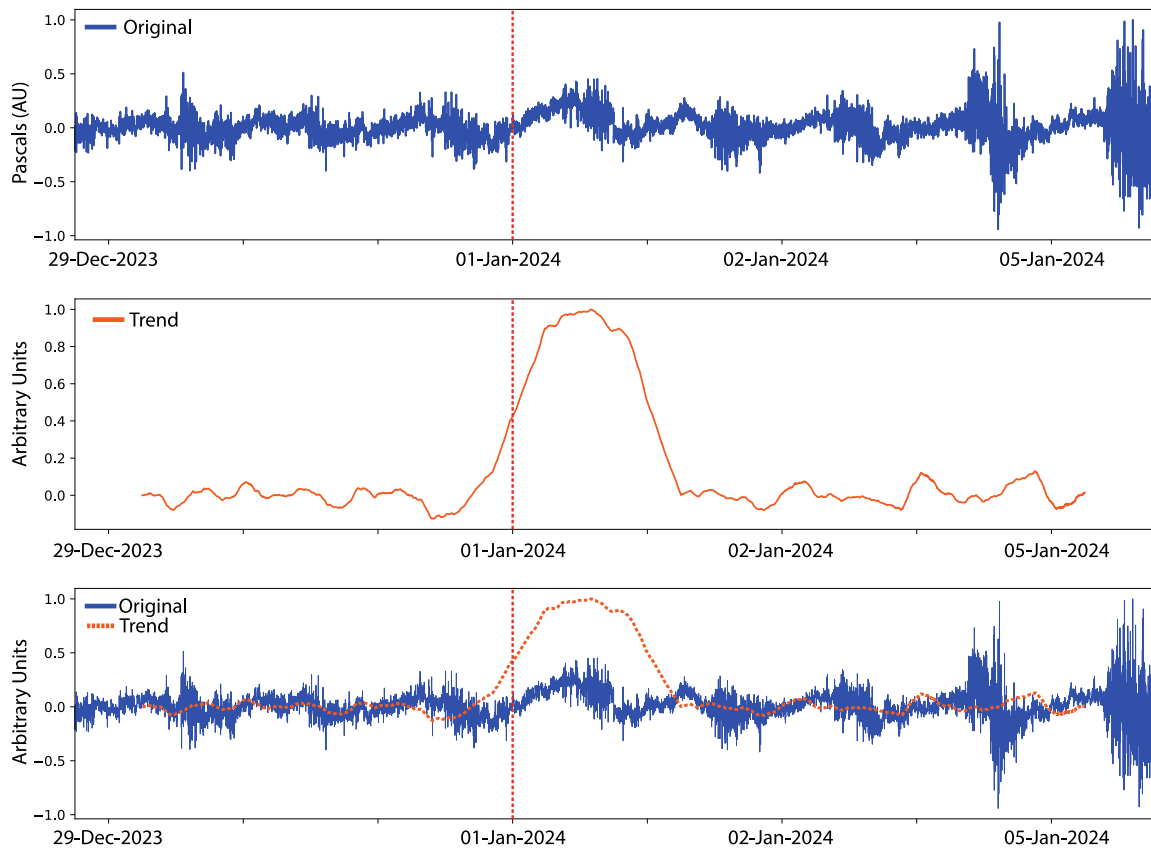
759

760 Figure 8

761

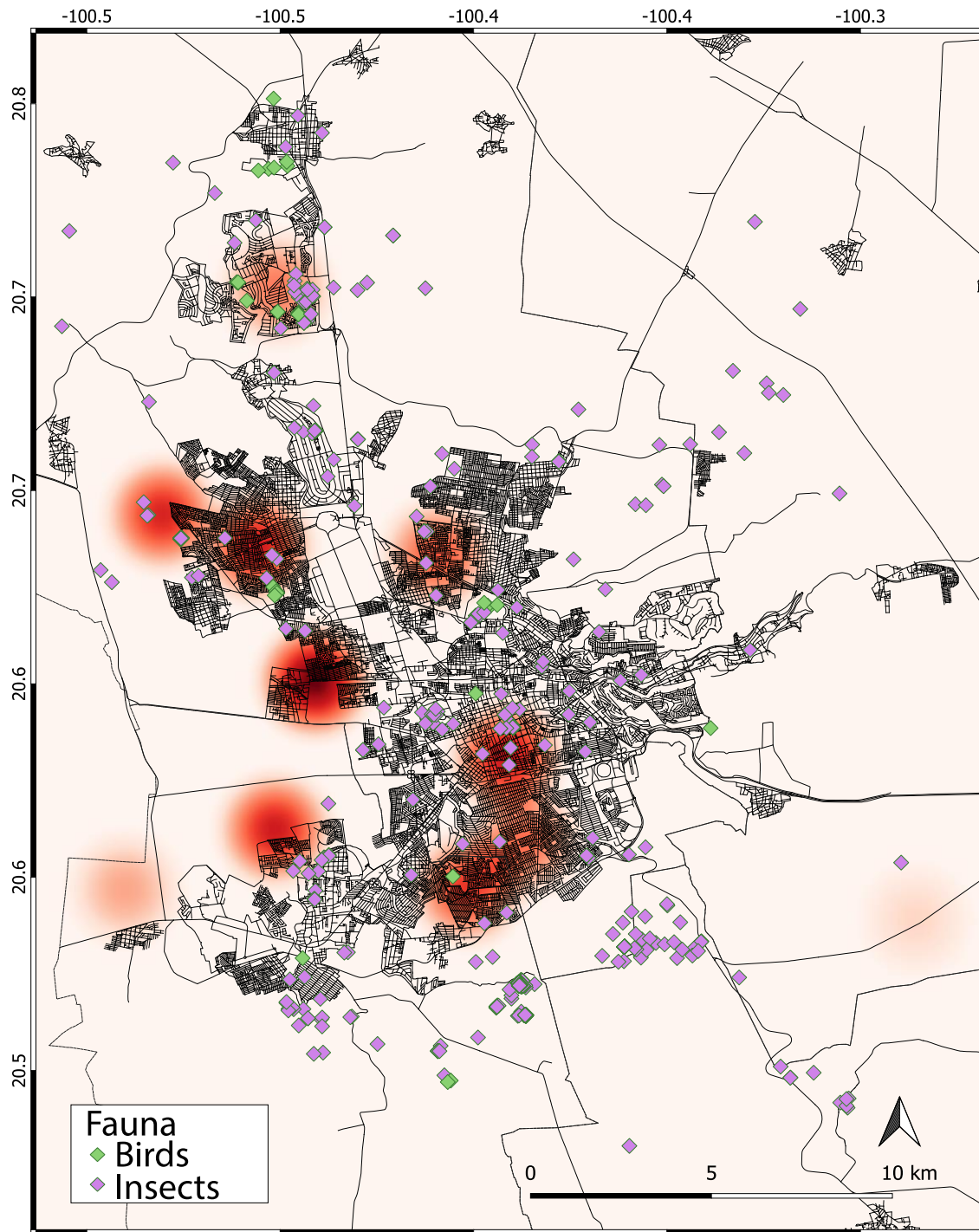
762

763



764

765 Figure 9



766

767 Figure 10